

Choroidal Thickness in Childhood

Scott A. Read, Michael J. Collins, Stephen J. Vincent, and David Alonso-Caneiro

Contact Lens and Visual Optics Laboratory, School of Optometry and Vision Science, Queensland University of Technology, Brisbane, Queensland, Australia

Correspondence: Scott A. Read, Contact Lens and Visual Optics Laboratory, School of Optometry and Vision Science, Queensland University of Technology, Room D517, O Block, Victoria Park Road, Kelvin Grove 4059, Brisbane, QLD, Australia; sa.read@qut.edu.au.

Submitted: January 24, 2013

Accepted: April 28, 2013

Citation: Read SA, Collins MJ, Vincent SJ, Alonso-Caneiro D. Choroidal thickness in childhood. *Invest Ophthalmol Vis Sci.* 2013;54:3586-3593. DOI:10.1167/iovs.13-11732

PURPOSE. We examined choroidal thickness (ChT) and its spatial distribution across the posterior pole in pediatric subjects with normal ocular health and minimal refractive error.

METHODS. ChT was assessed using spectral domain optical coherence tomography (OCT) in 194 children aged 4 to 12 years, with spherical equivalent refractive errors between +1.25 and -0.50 diopters sphere (DS). A series of OCT scans were collected, imaging the choroid along 4 radial scan lines centered on the fovea (each separated by 45°). Frame averaging was used to reduce noise and enhance chorioretinal junction visibility. The transverse scale of each scan was corrected to account for magnification effects associated with axial length. Two independent masked observers segmented the OCT images manually to determine ChT at foveal center, and averaged across a series of perifoveal zones over the central 5 mm.

RESULTS. The average subfoveal ChT was $330 \pm 65 \mu\text{m}$ (range, 189-538 μm), and was influenced significantly by age ($P = 0.04$). The ChT of the 4- to 6-year-old age group ($312 \pm 62 \mu\text{m}$) was significantly thinner compared to the 7- to 9-year-olds ($337 \pm 65 \mu\text{m}$, $P < 0.05$) and bordered on significance compared to the 10- to 12-year-olds ($341 \pm 61 \mu\text{m}$, $P = 0.08$). ChT also exhibited significant variation across the posterior pole, being thicker in more central regions. The choroid was thinner nasally and inferiorly compared to temporally and superiorly. Multiple regression analysis revealed age, axial length, and anterior chamber depth were associated significantly with subfoveal ChT ($P < 0.001$).

CONCLUSIONS. ChT increases significantly from early childhood to adolescence. This appears to be a normal feature of childhood eye growth.

Keywords: choroid, pediatric, optical coherence tomography, refractive error

The vascular choroid lines the posterior eye, and has a range of important and diverse anatomic and physiologic roles,¹ including supplying the outer retina with oxygen and nutrients,² ocular temperature regulation,³ the regulation of IOP,⁴ and the absorption of light.⁵ There also is evidence, primarily from research with animal models,⁶⁻⁸ that the choroid has an important role in the modulation of refractive state and may be involved in the development of refractive errors.

Improvements in noninvasive ocular imaging technology mean that the in vivo human choroid now can be imaged and measured reliably using Fourier domain OCT (FD-OCT).^{9,10} A number of recent studies using commercially available and custom developed FD-OCT devices have provided a range of new insights into the structural characteristics of the normal in vivo human choroid in adult populations.¹⁰⁻¹⁹ These studies have estimated the average thickness of the choroid in the subfoveal region of adults (over 18 years of age) with good ocular health to be between 192 and 354 μm . Regional differences in choroidal thickness across the posterior pole also have been reported in normal adults, with the choroid typically found to be thinner in regions nasal and inferior to the fovea.^{11,12,15,17} Studies also have documented a significant decrease in choroidal thickness of normal adult eyes with age^{10,11,13} and with increased levels of myopia/longer axial length.^{11,15,16,18} A variety of different ocular diseases, including retinitis pigmentosa,²⁰ central serous chorioretinopathy,²¹ age-related macular degeneration,²² diabetic retinopathy,²³ glaucoma,²⁴ and a range of different inherited retinal diseases,²⁵ also

have been found to be associated with changes in the thickness of the choroid.

Although the understanding of the characteristics of the in vivo choroid has increased substantially in recent years, to date only a few studies have examined the thickness of the choroid in children.²⁶⁻²⁸ Until recently, the main knowledge of choroidal thickness in childhood was derived primarily from histologic measures on postmortem eyes.²⁹ Three recent studies have used FD-OCT to examine the in vivo choroidal thickness in relatively small populations of children.²⁶⁻²⁸ These studies limited their assessment of choroidal thickness either to subfoveal locations only,²⁶ a series of discrete locations along a horizontal scan line,²⁸ or a horizontal and vertical scan line centered on the fovea.²⁷ An improved understanding of the characteristics of the normal thickness of the choroid in childhood should assist the diagnosis of choroidal abnormalities associated with eye disease, as well as understanding the changes that occur in the choroid associated with the normal growth of the eye, and in the development of refractive error. In our study we aimed to investigate the in vivo thickness of the choroid in a normal pediatric population, using high resolution FD-OCT, employing a scanning protocol that allows regional changes in choroidal thickness to be evaluated, accounting for transverse magnification effects associated with each subject's individual axial length. The latter correction was neglected in the three studies cited above. Given that previous studies have noted significant changes in choroidal thickness with refractive

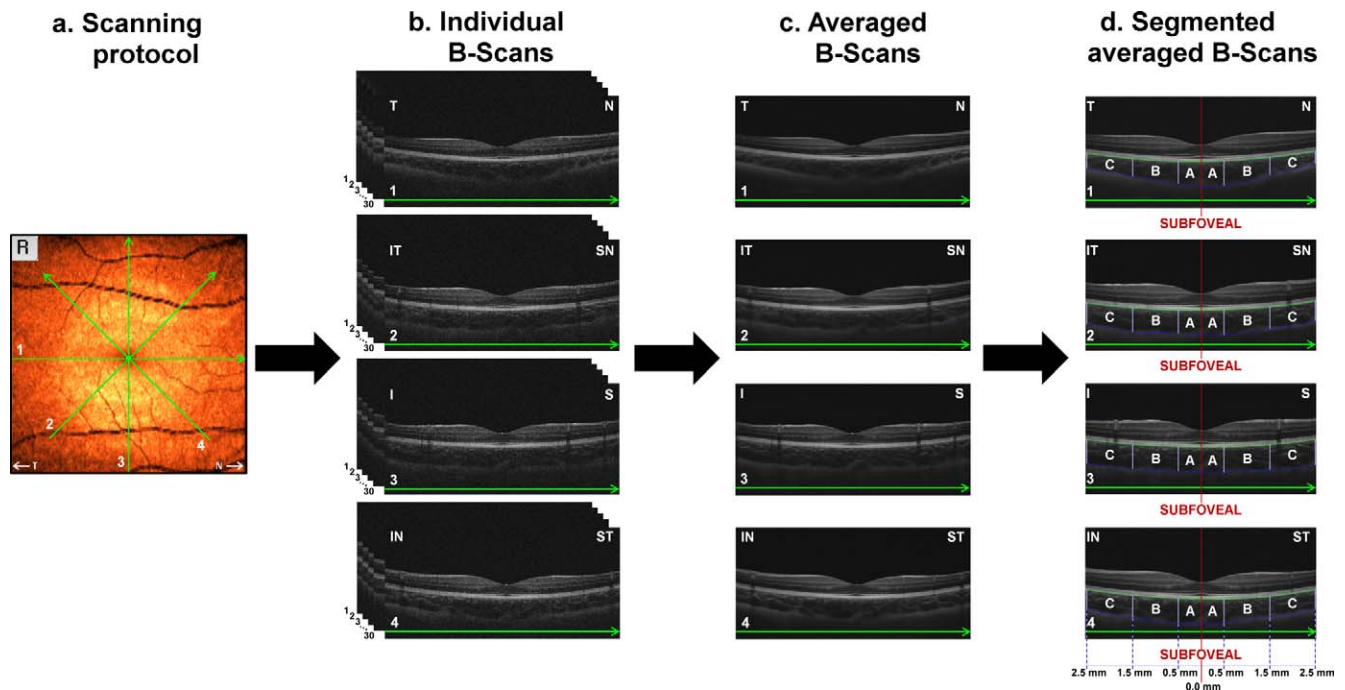


FIGURE 1. Overview of the OCT scanning protocol and image analysis performed on the OCT scans captured for each subject. OCT images from 4 radial scan lines centered on the fovea (a), each consisting of 30 individual B-scans (b) were captured. The individual B-scans from each scan line then were registered and averaged to create averaged B-scan images (c). Manual segmentation then defined the outer border of the RPE (green line in [d]) and inner border of the chorioscleral interface (blue line in [d]) in each image. The subfoveal choroidal thickness and average choroidal thickness within regions A (foveal region), B (parafoveal region), and C (perifoveal region) across the central 5 mm of the scan then were determined in each of the manually segmented averaged B-scans (d). Two experienced masked observers performed the manual segmentation.

error,^{30–33} in our study we have included only children with low levels of refractive error.

METHODS

Subjects and Procedures

All children ($n = 735$) attending a primary school in Brisbane, Australia, were invited to participate in our study. A total of 226 children aged 4 to 12 years agreed to participate. Approval from the Queensland University of Technology human research ethics committee was obtained before the study, and written informed consent was provided by all participating children and their parents. Any children who were too young to give written consent provided verbal assent to participate. All participants were treated in accordance with the tenets of the Declaration of Helsinki. All children underwent a series of vision screening tests to ascertain their visual acuity, ocular biometry, refraction, and ocular health status. These tests included measures of unaided and best corrected monocular visual acuity, noncycloplegic distance retinoscopy and subjective refraction, binocular vision measures, color vision screening, slit-lamp biomicroscopy, and 3D retinal OCT imaging. Ocular dimensions were measured using an optical biometer (Lenstar LS 900; Haag Streit AG, Koeniz, Switzerland), which is designed to measure with high precision, various ocular dimensions, including central corneal thickness (CCT), anterior chamber depth (ACD), lens thickness (LT), and axial length (AxL, defined as the distance from the anterior cornea to the retinal pigment epithelium).³⁴

Of the 226 children participating, 196 met the inclusion criteria of having a spherical equivalent refraction +1.25 to –1.25 diopters sphere (DS); normal visual acuity in both eyes

of 0.1 logMAR or better; no evidence of amblyopia or strabismus; no history of ocular disease, surgery, or injury; and no history of systemic disease or systemic medications with known ocular effects. Eligible children all had chorioretinal OCT images captured and analyzed to determine choroidal thickness. Of the 196 subjects included, the chorioscleral interface could not be detected reliably in the OCT scans of 2 subjects, whose data, thus, were not included in analyses.

The 194 children included in the final analysis of choroidal thickness had a mean \pm SD age of 8.2 ± 1.9 (range, 4–12 years) and 51% were female. Their mean spherical equivalent refraction was $+0.05 \pm 0.21$ (range, +1.25 to –0.50 DS), and the mean best corrected logMAR visual acuity was -0.04 ± 0.06 (range, 0.1 to –0.18). The majority of participating children were of Caucasian ethnic origin ($n = 176$), with the remaining children having East Asian ($n = 6$), Middle Eastern ($n = 5$), South American ($n = 3$), Melanesian ($n = 2$), or Indian ($n = 2$) ethnic origins.

Following the initial vision screening, each subject then had images of their posterior eye collected using a spectral domain OCT instrument (Copernicus SOCT-HR; Optopol Technology SA, Zawiercie, Poland). This instrument makes use of the principle of OCT, and includes a super-luminescent diode light source with a peak wavelength of 850 nm (bandwidth 100 nm). It offers an axial resolution of 3 μ m in retinal tissue, a transverse resolution of 12 to 18 μ m, and a scanning speed of 52,000 A-scans per second. Similar OCT devices have been found to provide reliable measurements of choroidal thickness.³⁵ For each subject, chorioretinal OCT scans were captured on one randomly selected eye only. Figure 1 illustrates the scanning protocol used in the study along with representative images from one subject. For these images, the instrument’s “chorioretinal” imaging mode was used (which focuses the instrument closer to the posterior

eye than the standard “vitreoretinal” imaging mode to enhance the signal from the choroid) in combination with the “cross” scanning protocol, which captures multiple sets of 2 perpendicular line scans centered on the fovea. For each OCT measurement, a series of “cross” scans were collected on each subject, including horizontal/vertical and 45°/135° “cross” scans. This scanning protocol resulted in the acquisition of 3 series of 4 radial line scans, each separated by 45°, and all centered on the fovea (Fig. 1a). Each of the line scans consisted of 30 B-scans, and 999 A-scans per B-scan. The 2 series of 4 radial line scans that exhibited the best image quality for each subject (as defined by the instruments’ quality index [QI], the clearest chorioretinal interface, and evidence of the most central fixation [deepest foveal pit]) were saved for additional analysis. Only OCT scans with an average image QI of $>4/10$ were included, as per the manufacturer’s instructions (average \pm SD QI from all measurements was 6.7 ± 1.1). Although detecting the chorioretinal boundary can be difficult in individual B-scans with QI values <5 , the improvement in image quality achieved by averaging multiple scans from the same individual (method described in detail below) allowed the RPE and chorioretinal interface to be detected reliably in all of the averaged images for our 194 subjects.

Data Analysis

Following the capture of the raw OCT images, custom written software was used to register and align the multiple B-scans along each scan line, to create averaged OCT images with reduced speckle noise, and enhanced visibility of the chorioretinal interface using a previously documented method.³⁶ These averaged images then were analyzed by two independent masked observers to manually segment the outer border of the RPE and the inner border of the chorioretinal interface across the 6 mm length of each scan to determine choroidal thickness. Each observer manually selected a series of points along the two boundaries, and a smooth function (a series of spline fits) then was fit automatically to these points to define the boundaries (initially the observers used 14 points along each boundary, but additional points could be added by the observers if the resulting line did not fit the boundary adequately). Each observer also manually selected the point in the image representing the center of the fovea (i.e., the deepest point of the central foveal pit). The results from the 2 observers then were averaged. The transverse scale of the scans also was adjusted based upon each subject’s axial length measurements to account for magnification factors associated with different eye sizes, using an approach similar to that of Wagner-Schuman et al.³⁷ Our method has been outlined in detail previously.³⁸

Based upon this analysis, the average subfoveal thickness was calculated in each image as the distance from the outer boundary of the RPE to the inner boundary of the chorioretinal interface at the center of the fovea. The average choroidal thickness within a series of different zones in the central 5 mm surrounding the fovea in each scan also was calculated. Figure 1d provides examples of segmented OCT images and an illustration of the different zones over which the choroidal thickness was averaged for each subject. The average thickness from foveal center to 0.5 mm away from the fovea was calculated (on either side of foveal center in each averaged scan) and was referred to as the “foveal” zone thickness. The average thickness from 0.5 mm away from foveal center to 1.5 mm from foveal center was calculated and referred to as the parafoveal zone thickness. The average thickness from 1.5 mm from the foveal center out to 2.5 mm on either side of the fovea was referred to as the perifoveal

zone choroidal thickness. Analysis of the images from the 4 radial scan lines for each subject, therefore, defined the choroidal thickness across the foveal, parafoveal, and perifoveal region in each of 8 different locations: temporal, superior-temporal, superior, superior-nasal, nasal, inferior-nasal, inferior, and inferior-temporal.

The choroidal thickness results from the two independent masked observers generally correlated closely and exhibited good agreement. For the subfoveal choroidal thickness, the interobserver correlation (R^2) was 0.99, with a mean interobserver difference of $-1 \pm 6 \mu\text{m}$ (95% limits of agreement, $+10$ to $-12 \mu\text{m}$). For all of the average thickness measures across each of the considered regions outside of the foveal center, the interobserver correlation was 0.96 with a mean difference of $+0.2 \pm 15 \mu\text{m}$ (95% limits of agreement, $+29$ to $-28 \mu\text{m}$).

A two-way ANOVA was performed to examine the influence of age and sex on subfoveal choroidal thickness (and ocular biometry) in the population. For this analysis, the subjects were divided into 3 groups based upon their age: 4- to 6-year-olds ($n = 57$), 7- to 9-year-olds ($n = 99$), and 10- to 12-year-olds ($n = 38$). Post hoc Tukey tests were used to explore between group differences. To examine the variation in choroidal thickness across the posterior pole, a repeated measures ANOVA was performed with two within-subjects factors (including choroidal location [temporal, superior-temporal, superior, superior-nasal, nasal, inferior-nasal, inferior, or inferior-temporal], and choroidal zone/region [foveal, parafoveal, and perifoveal]) and two between-subjects factors (age group and sex). Finally, stepwise multiple regression analysis was used to examine the influence of demographic (age and sex) and biometric (axial length, central corneal thickness, anterior chamber depth, and lens thickness) factors on subfoveal choroidal thickness. Only predictor variables contributing significantly to the regression model ($P < 0.05$) were included in the final model.

RESULTS

Subfoveal Choroidal Thickness

The mean subfoveal choroidal thickness for the entire population of 194 children was $330 \pm 65 \mu\text{m}$, ranging from 189 to 538 μm . ANOVA revealed a significant influence of age upon the subfoveal choroidal thickness ($P = 0.04$), with the subfoveal choroid of the 4- to 6-year-old age group (mean \pm SD thickness, $312 \pm 62 \mu\text{m}$) being thinner on average than the subfoveal choroidal thickness in the 7- to 9-year-old ($337 \pm 65 \mu\text{m}$) and 10- to 12-year-old ($341 \pm 61 \mu\text{m}$) age groups (Fig. 2a). The subfoveal choroidal thickness of the 4- to 6-year-olds was significantly thinner than the 7- to 9-year-olds on post hoc Tukey testing ($P < 0.05$), and bordered on significance when compared to the 10- to 12-year-olds ($P = 0.08$). The pattern of change in choroidal thickness appears to be defined by a relatively rapid increase in thickness in early childhood, followed by an apparent plateau in thickness change in older childhood (Fig. 2a). A similar pattern of thickness change with age also was observed when the data were stratified into 4 age groupings instead of 3 age groupings (data not shown). Univariate linear regression analysis revealed a highly significant positive association between subfoveal choroidal thickness and age (slope = 8.6, $r = 0.26$, $P < 0.001$, Fig. 2b). The average subfoveal choroidal thickness in the male subjects was $321 \pm 64 \mu\text{m}$ and in the female subjects it was $339 \pm 64 \mu\text{m}$; however, this difference in subfoveal choroidal thickness with sex did not reach statistical significance ($P = 0.2$). There was no significant sex by age interaction ($P = 0.4$).

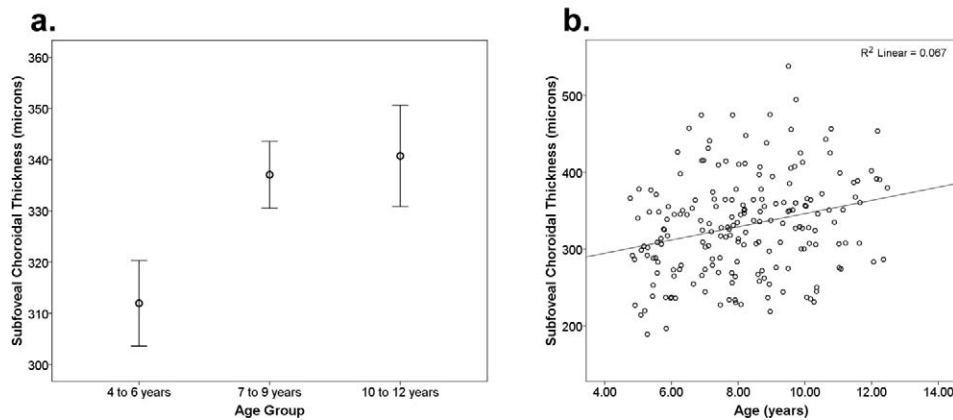


FIGURE 2. The influence of age upon subfoveal choroidal thickness. The average subfoveal choroidal thickness in the 4- to 6-year-old ($n = 57$), 7- to 9-year-old ($n = 99$), and 10- to 12-year-old ($n = 38$) age groups (a), and a scatter plot of subfoveal choroidal thickness with age (b). Error bars in (a) represent ± 1 SEM.

Topographical Choroidal Thickness

Table 1 and Figure 3 illustrate the topographic changes in choroidal thickness across the central 5 mm region surrounding the fovea. Repeated measures ANOVA revealed choroidal thickness to vary significantly with retinal region ($P < 0.001$). On average, the choroid was thickest in more central regions closer to the foveal center. The mean foveal region choroidal thickness ($329 \pm 64 \mu\text{m}$) was significantly thicker than the mean parafoveal choroidal thickness ($318 \pm 60 \mu\text{m}$), which was significantly thicker than the mean perifoveal choroidal thickness ($296 \pm 51 \mu\text{m}$, $P < 0.001$ for all comparisons). For the average of all subjects, the thickest choroid ($337 \pm 65 \mu\text{m}$) was located along the oblique scan line in a superior-temporal location, 0.9 mm from the foveal center. For the 4- to 6-year-old age group, the thickest choroid ($322 \pm 60 \mu\text{m}$) was located along the vertical scan line in a superior location, 1.5 mm from the foveal center. For the 7- to 9-year-olds the average thickest choroid ($344 \pm 63 \mu\text{m}$) was located along the oblique scan line in a superior-temporal location 0.8 mm from the foveal center. The thickest choroid of the 10- to 12-year-olds ($350 \pm 58 \mu\text{m}$) was located along the horizontal scan line in a temporal location 0.9 mm from the foveal center.

Significant variation in choroidal thickness also was noted with retinal location ($P < 0.001$), with the choroid being significantly thinner in nasal locations compared to temporal locations, and significantly thinner in inferior locations compared to superior locations ($P < 0.05$, all comparisons, Fig. 3a). A significant region by location interaction also was found ($P < 0.001$), which appears to be due to a more

prominent choroidal thinning in more peripheral regions observed in the nasal, superior-nasal, and inferior-nasal locations, compared to the other locations. Similar to the subfoveal data, the topographic choroidal thickness data also showed a significant influence of age ($P = 0.03$), with the younger age group (4-6-year-olds) exhibiting thinner choroids on average than the older age groups (Figs. 3b-d). There were no significant age by location or age by region interactions, suggesting a similar pattern of change with age in the different regions and locations. There was no significant influence of sex on the topographic choroidal thickness data ($P > 0.05$).

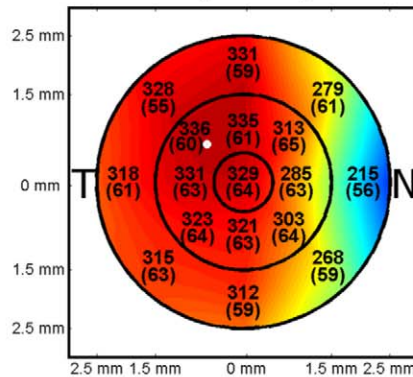
Ocular Biometry and Factors Associated With Choroidal Thickness

Table 2 illustrates the mean ocular biometric measurements for the 3 different age groups examined. Two-way ANOVA revealed a significant influence of age for all of the biometric variables examined (all $P < 0.05$). Significantly longer axial lengths, deeper anterior chambers, and thinner crystalline lenses were observed in the older age groups compared to the younger age groups ($P < 0.05$ for all post hoc comparisons). The 10- to 12-year-old children had significantly thicker corneas compared to the 7- to 9-year-old children (mean difference 0.015 mm, $P = 0.033$). Significant sex effects ($P < 0.05$) also were observed for a number of the biometric variables, with male subjects exhibiting significantly longer AxLs (mean AxL of 23.00 ± 0.75 mm in males and 22.55 ± 0.61 mm in females, $P < 0.001$), deeper anterior chambers (mean ACD of 3.03 ± 0.23 mm in males and 2.94 ± 0.23 mm in females, $P = 0.003$), and thicker

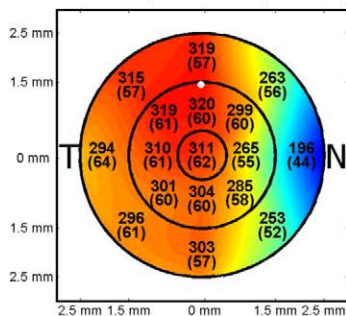
TABLE 1. Mean Choroidal Thickness for All Participating Children Averaged Across Each of the Choroidal Regions Within the Eight Different Locations Measured

	Mean \pm SD Choroidal Thickness, μm , $n = 194$			
	Foveal	Parafoveal	Perifoveal	Mean of All Regions
Temporal	333 \pm 64	331 \pm 63	318 \pm 61	327 \pm 63
Superior-temporal	334 \pm 64	336 \pm 60	328 \pm 55	333 \pm 60
Superior	332 \pm 64	335 \pm 61	331 \pm 59	333 \pm 61
Superior-nasal	329 \pm 65	313 \pm 65	279 \pm 61	307 \pm 67
Nasal	323 \pm 65	285 \pm 63	215 \pm 56	274 \pm 76
Inferior-nasal	325 \pm 65	303 \pm 64	268 \pm 59	299 \pm 67
Inferior	328 \pm 65	321 \pm 63	312 \pm 59	320 \pm 62
Inferior-temporal	329 \pm 65	323 \pm 64	315 \pm 63	322 \pm 64
Mean of all locations	329 \pm 64	318 \pm 60	296 \pm 51	

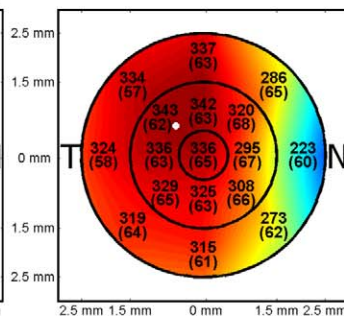
a. All subjects (n = 194)



b. 4 - 6 year olds (n = 57)



c. 7 - 9 year olds (n = 99)



d. 10 - 12 year olds (n = 38)

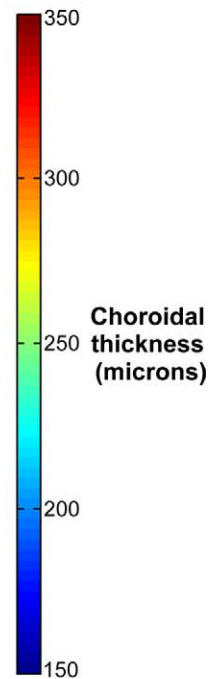
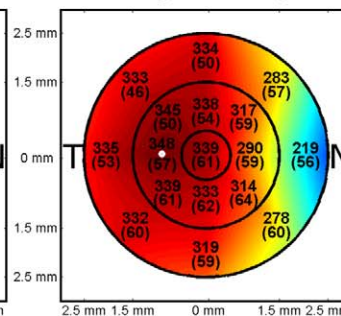


FIGURE 3. Topographic choroidal thickness maps, based upon the choroidal thickness data derived from the 4 radial line scans centered on the fovea, illustrating the average choroidal thickness across the central 5 mm region surrounding the fovea. The average choroidal thickness data for all subjects (a), and for the 4- to 6-year-old (b), 7- to 9-year-old (c), and 10- to 12-year-old (d) age groups is shown. The values on each of the maps indicate the mean choroidal thickness for each of the 8 measured locations, with the standard deviation in parentheses (note the value in the central foveal zone represents the average of all 8 locations). The *small white circle* on each map marks the average location of the thickest choroid in each of the maps.

corneas (mean CCT of 0.556 ± 0.033 mm males and 0.543 ± 0.033 mm in females, $P = 0.002$).

Stepwise multiple regression analysis to examine biometric (CCT, ACD, LT, and AxL) and demographic factors (age and sex) associated with subfoveal choroidal thickness revealed that age, AxL, and ACD all were associated significantly with choroidal thickness (Table 3). The final regression model, including these predictors, was highly statistically significant ($P < 0.001$), with a correlation coefficient (R) of 0.364. Age exhibited a positive association with subfoveal choroidal thickness ($B = 9.3$, $P < 0.001$) and appeared to be the strongest predictor in the model (inclusion of age increased the R^2 of the model by 0.06, $P = 0.003$). AxL exhibited a negative association with choroidal thickness ($B = -26.1$, $P = 0.001$), and its inclusion in the model increased the R^2 by 0.04 ($P = 0.015$). ACD was associated positively with choroidal thickness ($B = 59.7$, $P = 0.02$), and the inclusion of ACD increased the R^2 of the model by 0.04 ($P = 0.016$). None of the other considered

predictor variables contributed significantly to the variation observed in subfoveal choroidal thickness.

DISCUSSION

Only a limited number of studies have examined choroidal thickness in childhood, and to our knowledge, these choroidal thickness measures with OCT in our study represent the largest population of pediatric subjects to have in vivo choroidal thickness measurements assessed to date. In our population of 194 children aged 4 to 12 years, we found a mean subfoveal choroidal thickness of 330 μ m and, consistent with previous studies in adults,^{12,17} subfoveal choroidal thickness exhibited substantial variation between individuals. The three previous studies examining in vivo choroidal thickness with OCT in children have reported mean subfoveal choroidal thickness values of 337 μ m (from 23 Japanese

TABLE 2. Summary of the Mean Ocular Biometric Variables for the Population, Including CCT, ACD, LT, and AxL

	Mean Biometric Parameter, mm			
	4-6 y	7-9 y	10-12 y	Mean of All Subjects
CCT, n = 194	0.548 \pm 0.027	0.546 \pm 0.032	0.561 \pm 0.04	0.550 \pm 0.033
ACD, n = 193	2.89 \pm 0.25	3.01 \pm 0.20	3.05 \pm 0.25	2.99 \pm 0.23
LT, n = 149	3.66 \pm 0.19	3.52 \pm 0.16	3.49 \pm 0.13	3.56 \pm 0.18
AxL, n = 194	22.40 \pm 0.68	22.84 \pm 0.61	23.13 \pm 0.78	22.77 \pm 0.72

Note the ACD values are from 193 subjects and LT are from 149 subjects, as a reliable signal from the anterior lens was not visible in the biometry A-scan data for 1 subject and from the posterior lens for 45 subjects.

TABLE 3. Results From the Stepwise Multiple Regression Analysis Examining Biometric and Demographic Factors Associated With Subfoveal Choroidal Thickness

Predictor Variables	Unstandardized	Standardized	Significance (P)
	Coefficients B (SE)	Coefficients β	
Age	9.3 (2.7)	0.29	<0.001
AxL	-26.1 (8.0)	-0.30	0.001
ACD	59.7 (24.5)	0.22	0.02

R^2 of the regression model was 0.132 ($P < 0.001$).

children aged under 20 years),²⁶ 343 μm (from 30 Korean children aged 4-10 years),²⁷ and 313 μm (from 43 children aged 3-18 years),²⁸ which are in relatively close agreement with the values found in our current study. The use of a larger sample size of children with minimal refractive error, coupled with the scanning and analysis protocol used (including the correction of transverse magnification), allows our current study to provide a more detailed examination of the changes in choroidal thickness with age and the topographic changes in thickness across the central posterior pole in childhood than has been performed previously.

Fujiwara et al.²⁶ and Ruiz-Moreno et al.²⁸ both reported that children less than 10 years of age exhibited a thicker choroid compared to their other participants examined (children older than 10 years of age and adults); however, neither of these studies further stratified their pediatric subjects to examine age-related changes in choroidal thickness in early childhood. The use of a larger population of children in our current study has allowed us to examine the changes in choroidal thickness with age in younger children in more detail. This analysis showed that in early childhood (4-6 years) the choroid is significantly thinner than in the older age groups of children examined. The changes in choroidal thickness observed throughout childhood, as seen in Figure 2, appear to be characterized by a relatively rapid increase in early childhood, followed by a plateau in thickness change in the older age groups examined. Given that our pediatric population did not include children with significant refractive errors, this increase in choroidal thickness observed from early childhood to adolescence appears to be a characteristic associated with the eye's natural growth in childhood. A similar pattern of growth (i.e., rapid growth in early childhood, followed by a plateau in growth in adolescence) also has been described in emmetropic children for other ocular structures, including the anterior chamber and vitreous chamber.³⁹ Although to our knowledge this is the first study to report an increase in in vivo choroidal thickness from early childhood into adolescence in human eyes, two previous studies examining choroidal thickness changes in developing primates also have reported an increase in choroidal thickness associated with normal postnatal eye growth in macaques⁷ and marmosets.⁸

The exact mechanism underlying the changes observed in choroidal thickness in early childhood is not clear; however, the changes cannot be accounted for by a passive stretch mechanism with eye growth, as this would predict a thinning of the choroid rather than the observed thickening. Therefore, the thickening of the choroid may reflect normal growth in the vascular and connective tissue structure of the choroid, or alternatively could represent changes in blood flow with age. While changes in ocular blood flow have been documented in adults with age,^{40,41} to date ocular blood flow changes have not been examined in early childhood to our knowledge. Troilo et al. hypothesized that the thickening of the choroid observed in the normal development of the primate eye may function to

slow the growth of the eye during development, either by providing a barrier to diffusion of growth factors, or as a mechanical buffer to limit the eye's axial elongation.⁸ It is conceivable that the thickening of the choroid observed in our population of children could have a similar function to slow eye growth, given that the age at which the increases in choroidal thickness were observed appears to precede the age at which axial eye growth has been reported to slow in Caucasian emmetropic children.³⁹

One of the choroid's primary physiologic roles is to provide the outer retina with oxygen and nutrients.² Therefore, the changes in choroidal thickness that we have found with age in our population potentially could relate to changes in the structure and associated physiologic demands of the outer retina occurring with age. There is evidence from in vivo^{42,43} and histologic⁴⁴ studies that the central retina undergoes substantial changes postnatally and into childhood. Increases in the thickness of the central retina,^{42,43} changes in foveal morphology,^{42,43} and changes in photoreceptor characteristics (e.g., photoreceptor width, length, and packing density)⁴⁴ all have been documented to occur in normal growth from birth to childhood, with some studies suggesting that aspects of retinal morphology don't reach adult levels until the early teenage years.⁴⁴ The increased metabolic demand of a more densely packed foveal cone photoreceptor mosaic with age may be one factor related to the increased choroidal thickness we have observed from early childhood to adolescence.

A large number of recent studies have examined in vivo choroidal thickness in adults, and these studies have provided estimates of average subfoveal choroidal thickness ranging from 192 to 354 μm in a diversity of populations. There is clear evidence from a number of these cross-sectional studies that adult choroidal thickness undergoes significant decreases with aging and estimates of a mean decrease in choroidal thickness of 15 to 20 μm per 10 years of age^{10,12,26} have been made. A recent study examining choroidal thickness in Danish young adults aged in their 20s reported an average subfoveal choroidal thickness of 344 μm .¹⁶ Our finding of a mean choroidal thickness in our older children (aged 10-12 years) of 341 μm , suggests that by the age of 12 years, the choroidal thickness approaches adult values. Therefore, it appears that choroidal thickness increases from early childhood to adolescence, reaches a peak between 10 and 20 years of age, and then exhibits a gradual decrease into older adulthood.

Previous studies of choroidal thickness in children have reported only subfoveal thickness measures,²⁶ or have determined choroidal thickness at discrete points along a horizontal,²⁸ or a horizontal and vertical scan line through the fovea.²⁷ The scanning protocol used in our current study allows a more comprehensive examination of the spatial distribution of choroidal thickness across the posterior pole. On average, the thickest choroid was located slightly superiorly in the majority of subjects, but generally in relatively close proximity to the foveal center, and there was a tendency for the choroid to thin in more peripheral locations. The rate of thinning from center to more peripheral locations also exhibited significant inferior-superior and nasal-temporal asymmetries. A range of factors, such as the topographic characteristics of the retina, the influence of other ocular anatomic structures, and the eye's optical properties, all potentially could contribute to the regional changes in choroidal thickness observed across the central 5 mm of the posterior pole.

The increased metabolic demand of the outer retina associated with the high density of cone photoreceptors at the foveal center, and the peak in rod photoreceptor density typically that has been found to occur within the central 3 to 5 mm in the superior retina,^{45,46} may contribute to the increased choroidal thickness found in central and superior regions.

Previous studies^{12,17} in adults and children²⁷ also have noted the choroid to be slightly thicker in more superior locations. Anatomic restrictions related to the position of the posterior scleral foramen, and the entrance of the ciliary arteries and nerves into the posterior globe also are likely to contribute to aspects of observed regional changes in choroidal thickness, such as the prominent thinning of the choroid in nasal regions, which also has been a consistent finding in previous studies of adults^{10–15,17,18} and children.^{27,28} We also found evidence of a thinner choroid in inferior and inferior-nasal locations in our pediatric population. Previous studies that have mapped the distribution of choroidal thickness in adult subjects also have reported choroidal thinning in inferior-nasal locations.^{12,14,15,17} It has been hypothesized that the inferior-nasal thinning of the choroid may be related to the embryologic closure of the inferior fetal fissure in this general location.^{12,17} The fact that a thinner choroid in inferior-nasal locations also was observed in our population of children tends to support this theory. The optics of the eye also could influence the choroidal thickness characteristics, given the findings from animal research^{6–8} and recently from humans^{47,48} that optical defocus can induce changes in the thickness of the choroid. If optical defocus contributes to the topographic features of choroidal thickness, then it is more likely to be associated with asymmetric blur associated with higher order aberrations (such as vertical and horizontal coma) than more symmetrical blur associated with defocus and astigmatism, due to the asymmetric nature of the choroidal thickness changes from center to periphery. As only subjective refractions were measured in our study, further research involving measures of wavefront aberrations and choroidal thickness is required to address this issue.

Multiple regression analysis revealed that the two main predictors of subfoveal choroidal thickness in this population were age and axial length, with the significant positive association between age and choroidal thickness appearing to be the most important predictor. Axial length exhibited a negative correlation with choroidal thickness. Given that axial length also was found to be related strongly to age, a strong negative association between axial length and choroidal thickness would be expected to result in a decrease in choroidal thickness with age rather than the observed increase. However, the relationship between axial length and choroidal thickness in this population was weak, and was statistically significant only in the multiple regression analysis when age also was included in the model. Therefore, axial length and choroidal thickness exhibited a significant increase with age, but there was a tendency within each of the different age groups tested for longer eyes to exhibit thinner choroids. It should be noted that, although age and axial length were associated significantly with subfoveal choroidal thickness, the variation in demographic and biometric parameters examined in our study only account for a relatively small percentage (13%) of the variance in choroidal thickness in this population. Future studies examining a wider range of ocular and demographic parameters may help to understand better the factors influencing choroidal thickness in childhood.

A limitation of our current study is the cross-sectional design, which makes it difficult to attribute causation or to understand the time course of any changes. Longitudinal studies will help to clarify the time course of changes in choroidal thickness throughout childhood. None of our subjects exhibited significant refractive errors, thereby minimizing the potential confounding influence of refractive error on choroidal thickness. Previous findings in animal models indicate that significant choroidal thinning occurs during myopia development^{6–8} and a marked thinning of the choroid also has been found in adult human subjects with high myopia,^{30–33} which suggests a potentially important role for

the choroid in the development of refractive errors. Therefore, longitudinal studies of choroidal thickness in childhood, including myopic participants, will be important for improved understanding of the influence of refractive error upon choroidal thickness, and the temporal relationship between choroidal thickness changes, and the development and progression of childhood myopia. Such future studies should take account of the normal changes in choroidal thickness that we have found with age in our study.

In conclusion, we have examined the choroidal thickness of a relatively large population of children, without substantial refractive errors. We found a significant increase in choroidal thickness from early childhood into adolescence, which appears to be a normal feature of ocular growth. Future longitudinal studies will assist in clarifying the time course of change in choroidal thickness with age and the potential influence of refractive error development in childhood upon these changes.

Acknowledgments

The authors thank Payel Chatterjee for assistance with data collection and Beata Sander and Rod Jensen for assistance with data analysis procedures.

Supported by Australian Research Council “Discovery Early Career Research Award” DE120101434 (SAR).

Disclosure: **S.A. Read**, None; **M.J. Collins**, None; **S.J. Vincent**, None; **D. Alonso-Caneiro**, None

References

- Nickla DL, Wallman J. The multifunctional choroid. *Prog Retin Eye Res.* 2010;29:144–168.
- Bill A, Sperber G, Ujji K. Physiology of the choroidal vascular bed. *Int Ophthalmol.* 1983;6:101–107.
- Parver LM. Temperature modulating action of choroidal blood flow. *Eye.* 1991;5:181–185.
- Alm A, Nilsson FE. Uveoscleral outflow: a review. *Exp Eye Res.* 2009;88:760–768.
- Van Norren D, Tiemeijer LF. Spectral reflectance of the human eye. *Vision Res.* 1986;26:313–320.
- Wallman J, Wildsoet C, Xu A, et al. Moving the retina: choroidal modulation of refractive state. *Vision Res.* 1995;35:37–50.
- Hung LF, Wallman J, Smith EL. Vision-dependent changes in the choroidal thickness of macaque monkeys. *Invest Ophthalmol Vis Sci.* 2000;41:1259–1269.
- Troilo D, Nickla DL, Wildsoet CF. Choroidal thickness changes during altered eye growth and refractive state in a primate. *Invest Ophthalmol Vis Sci.* 2000;41:1249–1258.
- Spaide RF, Koizumi H, Pozzoni MC. Enhanced depth imaging spectral-domain optical coherence tomography. *Am J Ophthalmol.* 2008;146:496–500.
- Margolis R, Spaide R. A pilot study of enhanced depth imaging optical coherence tomography of the choroid in normal eyes. *Am J Ophthalmol.* 2009;147:811–815.
- Esmacelpour M, Považay B, Hermann B, et al. Three-dimensional 1060-nm OCT: choroidal thickness maps in normal subjects and improved posterior segment visualization in cataract patients. *Invest Ophthalmol Vis Sci.* 2010;51:5260–5266.
- Ikuno Y, Kawaguchi K, Nouchi T, Yasuno Y. Choroidal thickness in healthy Japanese subjects. *Invest Ophthalmol Vis Sci.* 2010;51:2173–2176.
- Manjunath V, Taha M, Fujimoto JG, Duker JS. Choroidal thickness in normal eyes measured using Cirrus HD optical coherence tomography. *Am J Ophthalmology.* 2010;150:325–329.

14. Ding X, Li J, Zeng J, et al. Choroidal thickness in healthy Chinese subjects. *Invest Ophthalmol Vis Sci.* 2011;52:9555–9560.
15. Hirata M, Tsujikawa A, Matsumoto A, et al. Macular choroidal thickness and volume in normal subjects measured by swept-source optical coherence tomography. *Invest Ophthalmol Vis Sci.* 2011;52:4971–4978.
16. Li XQ, Larsen M, Munch IC. Subfoveal choroidal thickness in relation to sex and axial length in 93 Danish university students. *Invest Ophthalmol Vis Sci.* 2011;52:8438–8441.
17. Ouyang Y, Heussen FM, Mokwa N, et al. Spatial distribution of posterior pole choroidal thickness by spectral domain optical coherence tomography. *Invest Ophthalmol Vis Sci.* 2011;52:7019–7026.
18. Chen FK, Yeoh J, Rahman W, Patel PJ, Tufail A, Da Cruz L. Topographic variation and interocular symmetry of macular choroidal thickness using enhanced depth imaging optical coherence tomography. *Invest Ophthalmol Vis Sci.* 2012;53:975–985.
19. Wei WB, Xu L, Jonas JB, et al. Subfoveal choroidal thickness: the Beijing Eye Study. *Ophthalmology.* 2013;120:175–80.
20. Dhoot DS, Huo S, Yuan A, et al. Evaluation of choroidal thickness in retinitis pigmentosa using enhanced depth imaging optical coherence tomography. *Br J Ophthalmol.* 2013;97:66–69.
21. Imamura Y, Fujiwara T, Margolis R, Spaide RF. Enhanced depth imaging optical coherence tomography of the choroid in central serous chorioretinopathy. *Retina.* 2009;29:1469–1473.
22. Manjunath V, Goren J, Fujimoto JG, Duker JS. Analysis of choroidal thickness in age-related macular degeneration using spectral-domain optical coherence tomography. *Am J Ophthalmol.* 2011;152:663–668.
23. Esmaelpour M, Považay B, Hermann B, et al. Mapping choroidal and retinal thickness variation in type 2 diabetes using three-dimensional 1060-nm optical coherence tomography. *Invest Ophthalmol Vis Sci.* 2011;52:5311–5316.
24. Maul EA, Friedman DS, Chang DS, et al. Choroidal thickness measured by spectral domain optical coherence tomography: factors affecting thickness in glaucoma patients. *Ophthalmology.* 2011;118:1571–1579.
25. Yeoh J, Rahman W, Chen F, et al. Choroidal imaging in inherited retinal disease using the technique of enhanced depth imaging optical coherence tomography. *Graefes Arch Clin Exp Ophthalmol.* 2010;248:1719–1728.
26. Fujiwara A, Shiragami C, Shirakata Y, Manabe S, Izumibata S, Shiraga F. Enhanced depth imaging spectral-domain optical coherence tomography of subfoveal choroidal thickness in normal Japanese eyes. *Jpn J Ophthalmol.* 2012;56:230–235.
27. Park KA, Oh SY. Analysis of spectral domain optical coherence tomography in preterm children: retinal layer thickness and choroidal thickness profiles. *Invest Ophthalmol Vis Sci.* 2012;53:7201–7207.
28. Ruiz-Moreno JM, Flores-Moreno I, Lugo, F, Ruiz-Medrano J, Montero JA, Akiba M. Macular choroidal thickness in normal pediatric population measured by swept-source optical coherence tomography. *Invest Ophthalmol Vis Sci.* 2013;54:353–359.
29. Ramrattan RS, van der Schaft TL, Mooy CM, de Bruijn WC, Mulder PG, de Jong PT. Morphometric analysis of Bruch's membrane, the choriocapillaris, and the choroid in aging. *Invest Ophthalmol Vis Sci.* 1994;35:2857–2864.
30. Fujiwara T, Imamura Y, Margolis R, Slakter JS, Spaide RF. Enhanced depth imaging optical coherence tomography of the choroid in highly myopic eyes. *Am J Ophthalmol.* 2009;148:445–450.
31. Ikuno Y, Tano Y. Retinal and choroidal biometry in highly myopic eyes with spectral-domain optical coherence tomography. *Invest Ophthalmol Vis Sci.* 2009;50:3876–3880.
32. Nishida Y, Fujiwara T, Imamura Y, Lima LH, Kurosaka D, Spaide RF. Choroidal thickness and visual acuity in highly myopic eyes. *Retina.* 2012;32:1229–1236.
33. Flores-Moreno I, Lugo F, Duker JS, Ruiz-Moreno JM. The relationship between axial length and choroidal thickness in eyes with high myopia. *Am J Ophthalmol.* 2013;155:314–319.
34. Buckhurst PJ, Wolffsohn JS, Shah H, Naroo SA, Davies LN, Berrow EJ. A new optical low coherence reflectometry device for ocular biometry in cataract patients. *Br J Ophthalmol.* 2009;93:949–953.
35. Benavente-Perez A, Hosking SL, Logan NS, Bansal D. Reproducibility-repeatability of choroidal thickness calculation using optical coherence tomography. *Optom Vis Sci.* 2010;87:867–872.
36. Alonso-Canerio D, Read SA, Collins MJ. Speckle reduction in optical coherence tomography imaging by affine-motion image registration. *J Biomed Opt.* 2011;16:116027.
37. Wagner-Schuman M, Dubis AM, Nordgren RN, et al. Race- and sex-related differences in retinal thickness and foveal pit morphology. *Invest Ophthalmol Vis Sci.* 2011;52:625–634.
38. Vincent SJ, Collins MJ, Read SA, Carney LG. Retinal and choroidal thickness in myopic anisometropia. *Invest Ophthalmol Vis Sci.* 2013;54:2445–2456.
39. Zadnik K, Mutti DO, Mitchell GL, Jones LA, Burr D, Moeschberger ML. Normal eye growth in emmetropic schoolchildren. *Optom Vis Sci.* 2004;81:819–828.
40. Ravalico G, Toffoli G, Pastori G, Crocè M, Calderini S. Age-related ocular blood flow changes. *Invest Ophthalmol Vis Sci.* 1996;37:2645–2650.
41. Straubhaar M, Orgül S, Gugleta K, Schötzau A, Erb C, Flammer J. Choroidal laser Doppler flowmetry in healthy subjects. *Arch Ophthalmol.* 2000;118:211–215.
42. Maldonado RS, O'Connell RV, Sarin N et al. Dynamics of human foveal development after premature birth. *Ophthalmology.* 2011;118:2315–2325.
43. Vajzovic L, Hendrickson AE, O'Connell RV, et al. Maturation of the human fovea: correlation of spectral-domain optical coherence tomography findings with histology. *Am J Ophthalmol.* 2012;154:779–789.
44. Hendrickson A, Possin D, Vajzovic L, Toth CA. Histologic development of the human fovea from midgestation to maturity. *Am J Ophthalmol.* 2012;154:767–778.
45. Curcio CA, Sloan KR, Kalina RE, Hendrickson AE. Human photoreceptor topography. *J Comp Neurol.* 1990;292:497–523.
46. Hendrickson A, Drucker D. The development of parafoveal and mid-peripheral human retina. *Behav Brain Res.* 1992;49:21–31.
47. Read SA, Collins MJ, Sander BP. Human optical axial length and defocus. *Invest Ophthalmol Vis Sci.* 2010;51:6262–6269.
48. Chakraborty R, Read SA, Collins MJ. Monocular myopic defocus and daily changes in axial length and choroidal thickness of human eyes. *Exp Eye Res.* 2012;103:47–54.